Journal of Sound and Vibration (2000) **236**(1), 115–128
doi:10.1006/jsvi.2000.2964, available online at http://www.idealibrary.com on IDEAL®

THREE-DIMENSIONAL RESPONSE AND INTENSITY OF TORSIONAL VIBRATION IN A STEPPED SHAFT

J. Q. PAN

Department of Instrumentations Science and Engineering, Zhejiang University,. Hangzhou 310027, *People's Republic of China*

AND

J. PAN, R. S. MING AND T. LIN

Department of Mechanical and Materials Engineering, The University of Western Australia, Nedlands W A 6907, *Australia*

(*Received* 19 *July* 1999, *and in final form* 10 *February* 2000)

In this paper, a method is presented for predicting the three-dimensional dynamic response, shear stresses and structural intensity of torsional vibration in a finite shaft with stepped cross-sections. The series expansion techniques is employed to express the dynamic responses and shear stresses in terms of the eigenfunctions of torsional vibration in uniform cylindrical rods. The coefficients of the series are determined by enforcing the boundary conditions through the least-squares fitting. The effectiveness of this proposed method is assessed and illustrated by numerical results. The numerical results also revealed the characteristics of dynamic response, shear stresses and intensity vector fields in a finite stepped shaft and showed that the application of the one-dimensional torsional vibration theory to a finite stepped shaft not only misses out radial modal responses, but also results in a large error for the prediction of responses of axial modes when the resonance frequencies of all the segments (in free–free end conditions) do not coincide.

1. INTRODUCTION

Shafts including stepped shafts are elements of many practical engineering structures. Torsional vibration problems often arise in these elements and they are usually analyzed based on one-dimensional mathematical models [1]. However, one-dimensional mathematical models can only give approximate results [2, 3] and the approximation error increases with increasing frequency. At low frequencies where the velocities of elements in a given cross-section of a shaft are all in the same (tangential) direction and their magnitudes are proportional to the radius, the one-dimensional model is a good approximation. At medium and high frequencies where the torsional wavelengths are comparable with or smaller than the radius of a shaft, radial vibrational modes are present and the accurate analysis of torsional vibration in a shaft should be made based on three-dimensional mathematical models because the tangential displacement in any cross-section of the shaft may not be a linear function of radius, and one or more radial layers may rotate in opposite direction to that of the core of the shaft.

A number of researchers have used three-dimensional methods to study the torsion vibration in shaft [2–8]. Leissa and So [2] used the three-dimensional Ritz analysis to

0022-460X/00/360115 + 14 $35.00/0

estimate the resonance frequencies of finite shafts and concluded that a three-dimensional mathematical model is required to obtain an accurate estimation of natural frequencies. Pan and Pan [3] studied the structural intensity of torsional vibration in uniform shafts and demonstrated the torsional energy flow features at medium and high frequencies where an one-dimensional mathematical model is in error. Johnson *et al.* [4] used a three-dimensional mathematical model to look at the trapped torsional modes in a stepped shaft of three segments. Tsuji and Kim [5–8] utilized three-dimensional methods to analyze the stress field of infinite stepped shafts and showed stress singularity phenomena cannot be explained by using the one-dimensional torsional vibration theory. In reference [8], the tangential displacement and shear stresses of a stepped shaft with two semi-infinite solid cylindrical rods are expressed in terms of Dini series [9]. The Dini-series coefficients are then determined using the boundary conditions at the stepped joint. The advantage of this approach manifests itself in concise formulation and in actual numerical calculation efficiency because it involves no numerical integration.

Practical shafts are all finite and could be of a large cross-section or consists of several segments with different radii. The study of torsional vibration in such stepped shaft may provide a understanding of the characteristics of torsional modes in complex structures and an information for machinery vibration and noise control. In this paper, a three-dimensional method is proposed for obtaining numerical solutions of torsional response, shear stresses and structural intensity in a stepped shaft with two segments for the excitation of a pure torsional moment due to axial symmetrical surface forces. The similarity of this proposed method and the method developed in reference [8] is that in both methods the expressions of tangential displacement and shear stresses are analytic (in terms of Dini series, the exact eigenfunctions of torsion vibration in uniform cylindrical rods) and have no integration terms. The difference is that in this proposed method the Dini coefficients are obtained by directly applying the method of least squares [10] to fit the boundary conditions at the stepped joint. This proposed method is readily extended to the case where a stepped shaft consists of several segments of different radii and has different boundary conditions.

2. TORSIONAL VIBRATION IN A STEPPED SHAFT

We consider a stepped shaft which consists of two uniform solid cylindrical rods (segments) of different finite lengths and diameters. The axis of the stepped shaft is lying along the z-axis of a cylindrical co-ordinate system (r, θ, z), as shown in Figure 1. The radii and lengths of the two segments are denoted by R_1, $R_2 (R_1 > R_2)$, L_1 and L_2 respectively. The stepped shaft is assumed to have free–free end conditions. An axial-symmetrically distributed surface force, $\Theta_0 \, e^{j\omega t}$, is assumed to act on the left end of the shaft ($z = 0$) in the tangential direction resulting in a harmonic torque $M_0 \, e^{j\omega t}$:

$$M_0 = \int_0^{2\pi} \int_0^{R_1} r \Theta_0(r) \, ds, \tag{1}$$

where $ds = r dr \, d\theta$. For this type of excitation, only torsional waves are present in the shaft [3]. Due to the circular cross-sections, the tangential displacements in segments 1 and 2 of the shaft should be independent of θ and can be expressed respectively as [2, 3]

$$v_i(r, z, t) = \left\{ r \left[A_0^{(i)} e^{jk_0^{(i)} z} + B_0^{(i)} e^{jk_0^{(i)} z} \right] + \sum_{n=1}^{\infty} J_1(\beta_n^{(i)} r) \left[A_n^{(i)} e^{jk_n^{(i)} z} + B_n^{(i)} e^{-jk_n^{(i)} z} \right] \right\} e^{j\omega t}, \quad i = 1,2, \tag{2}$$

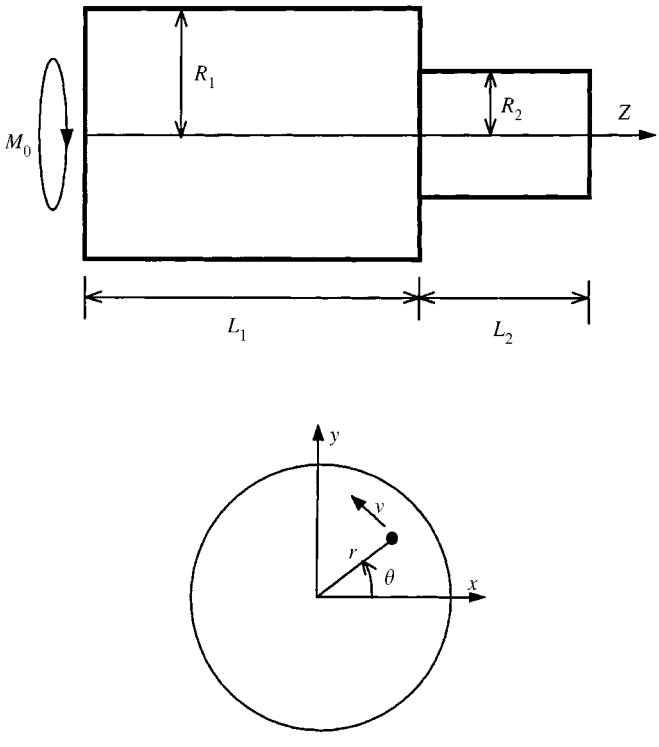

Figure 1. A shaft with two cross-sections and the corresponding co-ordinates.

where

$$k_0^{(i)} = \omega \sqrt{\frac{\rho_i}{G_i}}, \qquad k_n^{(i)} = \sqrt{\frac{\rho_i \omega^2}{G_i} - (\beta_n^{(i)})^2}, \quad n = 1,2, \ldots \cdot \tag{3}$$

$\beta_n^{(1)}$ and $\beta_n^{(2)}$ are the eigenvalues in the radial direction satisfying the eigenequations:

$$\mathrm{J}_2(\beta^{(i)} R_i) = 0, \quad i = 1,2. \tag{4}$$

J_1 and J_2 are, respectively, the first and second order Bessel functions of the first kind, ρ_i is the material density, $G_i = G_0^{(i)}(1 + \mathrm{j}\eta_i)$ is the complex shear modulus and η_i is the dissipation loss factor of segment i. The coefficients $A_0^{(i)}$, $A_1^{(i)}$, … and $B_0^{(i)}$, $B_1^{(i)}$, … in equation (2) are determined by the boundary conditions at the two ends of each segment. For the stepped shaft shown in Figure 1, the boundary conditions can be written as the following four equations:

$$G_1 \frac{\partial v_1}{\partial z} = -\Theta_0(r)\,\mathrm{e}^{\mathrm{j}\omega t}, \quad \text{at } z = 0, \tag{5}$$

$$G_1 \frac{\partial v_1}{\partial z} = \Theta_1(r)\,\mathrm{e}^{\mathrm{j}\omega t}, \quad \text{at } z = L_1, \tag{6}$$

$$G_2 \frac{\partial v_2}{\partial z} = -\Theta_2(r)\,\mathrm{e}^{\mathrm{j}\omega t}, \quad \text{at } z = L_1, \tag{7}$$

$$G_2 \frac{\partial v_2}{\partial z} = 0; \quad \text{at } z = L = L_1 + L_2, \tag{8}$$

where $\Theta_1(r)$ and $\Theta_2(r)$ are the internal shear forces at the stepped joint in the tangential direction. The force equilibrium at the stepped joint requires $\Theta_1 = -\Theta_2$ $(r \leqslant R_2)$ and $\Theta_1 = 0$ $(R_2 \leqslant r \leqslant R_1)$.

Substituting equation (2) into equations (5)–(8) gives

$$v_1(r, z, t) = -\left\{ \begin{array}{l} \dfrac{r}{G_1 k_0^{(1)} N_0^{(1)} \sin(k_0^{(1)} L_1)} \left[H_0^{(1)} \cos(k_0^{(1)} z) + H_0^{(0)} \cos(k_0^{(1)}(z - L_1))\right] \\ + \displaystyle\sum_{n=1}^{\infty} \dfrac{\mathrm{J}_1(\beta_n^{(1)} r)}{G_1 k_n^{(1)} N_n^{(1)} \sin(k_n^{(1)} L_1)} + \left[H_n^{(1)} \cos(k_n^{(1)} z) + H_n^{(0)} \cos(k_n^{(1)}(z - L_1))\right] \end{array} \right\} e^{\mathrm{j}\omega t}, \tag{9}$$

$$v_2(r, z, t) = -\left\{ \frac{r H_0^{(2)} \cos(k_0^{(2)}(z - L))}{G_2 k_0^{(2)} N_0^{(2)} \sin(k_0^{(2)} L_2)} + \sum_{n=1}^{\infty} \frac{J_1(\beta_n^{(2)} r) H_n^{(2)} \cos(k_n^{(2)}(z - L))}{G_2 k_n^{(2)} N_n^{(2)} \sin(k_n^{(2)} L_2)} \right\} \mathrm{e}^{\mathrm{j}\omega t}, \tag{10}$$

where

$$N_0^{(1)} = \frac{R_1^4}{4}, \quad N_0^{(2)} = \frac{R_2^4}{4}, \quad N_n^{(1)} = \frac{R_1^2 J_1^2(\beta_n^{(1)} R_1)}{2}, \quad N_n^{(2)} = \frac{R_2^2 J_1^2(\beta_n^{(2)} R_2)}{2}, \tag{11}$$

$H_0^{(0)}$, $H_0^{(1)}$, $H_0^{(2)}$ and $H_n^{(0)}$, $H_n^{(1)}$, $H_n^{(2)}$ $(n = 1,2,3, \ldots)$ are the modal moments and given by the following integrals:

$$H_0^{(0)} = \int_0^{R_1} \Theta_0 r^2 \,\mathrm{d}r, \quad H_0^{(1)} = \int_0^{R_1} \Theta_1 r^2 \,\mathrm{d}r, \quad H_0^{(2)} = \int_0^{R_2} \Theta_2 r^2 \,\mathrm{d}r, \tag{12}$$

$$H_n^{(0)} = \int_0^{R_1} \Theta_0 \mathrm{J}_1(\beta_n^{(1)} r) r \,\mathrm{d}r, \quad H_n^{(1)} = \int_0^{R_1} \Theta_1 \mathrm{J}_1(\beta_n^{(1)} r) r \,\mathrm{d}r,$$

$$H_n^{(2)} = \int_0^{R_2} \Theta_2 \mathrm{J}_1(\beta_n^{(2)} r) r \,\mathrm{d}r. \tag{13}$$

The internal shear forces $\Theta_1(r)$ and $\Theta_2(r)$ can be expanded in Fourier–Bessel series:

$$\Theta_i(r) = c_0^{(i)} r + \sum_{n=1}^{\infty} c_n^{(i)} \mathrm{J}_1(\beta_n^{(i)} r), \quad i = 1, 2, \tag{14}$$

where $c_0^{(i)}$, $c_1^{(i)}$, $c_2^{(i)}$, … are the Fourier–Bessel coefficients of the internal shear force $\Theta_i(r)$. Substituting the above equation into equations (12) and (13) and using the orthogonal property of the functions $\{r, \mathrm{J}_1(\beta_n^{(1)} r)\}$ over interval $[0, R_1]$ and that of $\{r, \mathrm{J}_1(\beta_n^{(2)} r)\}$ over interval $[0, R_2]$ five the following relationships:

$$H_0^{(i)} = c_0^{(i)} N_0^{(i)}, \qquad H_n^{(i)} = c_n^{(i)} N_n^{(i)}, \quad i = 1, 2 \tag{15}$$

By using the above relationships, equations (9) and (10) can be simplified as

$$v_1(r, z, t) =$$

$$-\left\{\begin{array}{l}\dfrac{r}{G_1 k_0^{(1)} \sin(k_0^{(1)} L_1)}\ [c_0^{(1)} \cos(k_0^{(1)} z) + c_0^{(0)} \cos(k_0^{(1)}(z - L_1))] \\ \quad + \displaystyle\sum_{n=1}^{\infty} \frac{\mathrm{J}_1(\beta_n^{(1)} r)}{G_1 k_n^{(1)} \sin(k_n^{(1)} L_1)} + [c_n^{(1)} \cos(k_n^{(1)} z) + c_n^{(0)} \cos(k_n^{(1)}(z - L_1))]\end{array}\right\} e^{\mathrm{j}\omega t}, \tag{16}$$

$$v_2(r, z, t) = -\left\{\frac{r c_0^{(2)} \cos(k_0^{(2)}(z - L))}{G_2 k_0^{(2)} \sin(k_0^{(2)} L_2)} + \sum_{n=1}^{\infty} \frac{J_1(\beta_n^{(2)} r) c_n^{(2)} \cos(k_n^{(2)}(z - L))}{G_2 k_n^{(2)} \sin(k_n^{(2)} L_2)}\right\} \mathrm{e}^{\mathrm{j}\omega t}, \tag{17}$$

where $\Theta_0(r) = c_0^{(0)} r + \sum_{n=1}^{\infty} c_n^{(0)} \mathrm{J}_1(\beta_n^{(1)} r)$ and $c_n^{(0)} = H_n^{(0)} / N_n^{(0)}$ ($n = 1,2,3, \ldots$).

The Fourier–Bessel coefficients can be determined from the boundary conditions at the stepped joint ($z = L_1$) where the displacement continuity and force equilibrium must be satisfied. That is

$$v_1(r, L_1, t) = v_2(r, L_1, t), \quad 0 \leqslant r \leqslant R_2, \tag{18}$$

$$\frac{\partial v_1(r, L_1, t)}{\partial z} = 0, \quad R_2 \leqslant r \leqslant R_1, \tag{19}$$

$$G_1 \frac{\partial v_1(r, L_1, t)}{\partial z} = G_2 \frac{\partial v_2(r, L_1, t)}{\partial z}, \quad 0 \leqslant r \leqslant R_2. \tag{20}$$

Substituting equations (16) and (17) into the above equations gives

$$\frac{r \cos(k_0^{(1)} L_1)}{G_1 k_0^{(1)} \sin(k_0^{(1)} L_1)} c_0^{(1)} + \sum_{n=1}^{\infty} \frac{\mathrm{J}_1(\beta_n^{(1)} r) \cos(k_n^{(1)} L_1)}{G_1 k_n^{(1)} \sin(k_n^{(1)} L_1)} c_n^{(1)} - \frac{r \cos(k_0^{(2)} L_2)}{G_2 k_0^{(2)} \sin(k_0^{(2)} L_2)} c_0^{(2)}$$

$$- \sum_{n=1}^{\infty} \frac{\mathrm{J}_1(\beta_n^{(2)} r) \cos(k_n^{(2)} L_2)}{G_2 k_n^{(2)} \sin(k_n^{(2)} L_2)} c_n^{(2)} = -\frac{r c_0^{(0)}}{G_1 k_0^{(1)} \sin(k_0^{(1)} L_1)}$$

$$- \sum_{n=1}^{\infty} \frac{\mathrm{J}_1(\beta_n^{(1)} r) c_n^{(0)}}{G_1 k_n^{(1)} \sin(k_n^{(1} L_1)}, \quad 0 \leqslant r \leqslant R_2\,. \tag{21}$$

$$r c_0^{(1)} + \sum_{n=1}^{\infty} \mathrm{J}_1(\beta_n^{(1)} r) c_n^{(1)} = 0, \quad R_2 \leqslant r \leqslant R_1, \tag{22}$$

$$r c_0^{(1)} + \sum_{n=1}^{\infty} \mathrm{J}_1(\beta_n^{(1)} r) c_n^{(1)} + r c_0^{(2)} + \sum_{n=1}^{\infty} \mathrm{J}_1(\beta_n^{(2)} r) c_n^{(2)} = 0, \quad 0 \leqslant r \leqslant R_2, \tag{23}$$

where the coefficients $c_n^{(i)}$ ($i = 1,2$; $n = 1, 2, 3, \ldots$) can be approximately estimated using the method of least squares. By using the method of least squares, equations (21)–(23) are satisfied only at a limit number of locations. If $(P + Q + 2)$ coefficients, $c_n^{(1)}$ ($n = 0, 1, 2, \ldots, P$) and $c_n^{(2)}$ ($n = 0,1,2, \ldots, Q$), are used to describe the internal shear forces at the stepped joint, and equations (21)–(23) are satisfied at $(M + N)$ locations ($r = r_1, r_2, \ldots, r_M, r_{M+1}, r_{M+2}, \ldots, r_{M+N}$) on the right end of segment 1 and at M locations ($r = r_1, r_2, \ldots, r_M$) on left end of segment 2, the following matrix equation can be obtained:

$$[\Delta][c] = [d], \tag{24}$$

where $[c] = [c_0^{(1)}\ c_1^{(1)}\ \cdots\ c_P^{(1)}\ c_0^{(2)}\ c_1^{(2)}\ \cdots\ c_Q^{(2)}]^{\mathrm{T}}$ is the Fourier–Bessel coefficient vector; $[d] = [d_1\ d_2\ \cdots\ d_{2M+N}]^{\mathrm{T}}$ is the external moment vector, of which the element are given by

$$d_s = \begin{cases} -\dfrac{r_s c_c^{(0)}}{G_1 k_0^{(1)} \sin(k_n^{(1)} L_1)} - \displaystyle\sum_{n=1}^{S} \frac{\mathrm{J}_1(\beta_n^{(1)} r_s)\, c_n^{(0)}}{G_1 k_n^{(1)} \sin(k_n^{(1)} L_1)} & (s = 1,2, \ldots, M) \\ 0 & (s = M+1, M+2, \ldots, 2M+N), \end{cases} \tag{25}$$

where S is the maximum number of base functions used in the calculation of tangential displacement in segment I. The coefficient matrix $[\Delta]$ in equation (24) has an order of $(2M+N)\times(P+Q+2)$ and its elements are given by

$$\Delta_{ij} = \begin{cases} \dfrac{r_i \cos(k_0^{(1)} L_1)}{G_1 k_0^{(1)} \sin(k_0^{(1)} L_1)} & (i = 1,2, \ldots, M;\ j = 1), \\ \dfrac{\mathrm{J}(\beta_{j-1}^{(1)} r_i) \cos(k_{j-1}^{(1)} L_1)}{G_1 k_{j-1}^{(1)} \sin(k_{j-1}^{(1)} L_1)} & \begin{pmatrix} i = 1,2, \ldots, M \\ j = 2,3, \ldots, P+1 \end{pmatrix}, \\ \dfrac{r_i \cos(k_0^{(2)} L_2)}{G_2 k_0^{(2)} \sin(k_0^{(2)} L_2)} & (i = 1,2, \ldots, M;\ j = P+2), \\ \dfrac{\mathrm{J}_1(\beta_{j-P-2}^{(2)} r_s) \cos(k_{j-P-2}^{(2)} L_2)}{G_2 k_{j-P-2}^{(2)} \sin(k_{j-P-2}^{(2)} L_2)} & \begin{pmatrix} i = 1,2, \ldots, M \\ j = P+3, \ldots, P+Q+2 \end{pmatrix}, \end{cases} \tag{26a}$$

$$\Delta_{ij} = \begin{cases} r_i & \begin{pmatrix} i = M+1, \ldots, M+N \\ j = 1 \end{pmatrix}, \\ \mathrm{J}_1(\beta_{j-1}^{(1)} r_i) & \begin{pmatrix} i = M+1, \ldots, M+N \\ j = 2,\ 3, \ldots, P+1 \end{pmatrix}, \\ 0 & \begin{pmatrix} i = M+1, \ldots, M+N \\ j = P+2, \ldots, P+Q+2 \end{pmatrix}, \end{cases} \tag{26b}$$

$$\Delta_{ij} = \begin{cases} r_i & (i = M+N+1, \ldots, 2M+N;\ j = 1), \\ \mathrm{J}_1(\beta_{j-1}^{(1)} r_i) & \begin{pmatrix} i = M+N+1, \ldots, 2M+N \\ j = 2,3, \ldots, P+1 \end{pmatrix}, \\ r_i & (i = M+N+1, \ldots, 2M+N;\ j = P+2), \\ \mathrm{J}_1(\beta_{j-P-1}^{(2)} r_i) & \begin{pmatrix} i = M+N+1, \ldots, 2M+N \\ j = P+3, \ldots, P+Q+2 \end{pmatrix}. \end{cases} \tag{26c}$$

If the coefficient matrix $[\Delta]$ is singular, the least-squares solution of equation (24) can be expressed as

$$[c] = ([\Delta]^{\mathrm{T}}[\Delta])^{-1}\ [\Delta]^{\mathrm{T}}\ [d]. \tag{27}$$

Substituting the above solution into equations (16) and (17) gives the torsional response of the stepped shaft. Then the internal shear stresses can also be calculated [3].

3. STRUCTURAL INTENSITY OF TORSIONAL VIBRATION

Structural intensity vector $I = [I_r, I_\theta, I_z]^T$ in an elastic structure is defined as [11, 12]

$$I = \begin{bmatrix} I_r \\ I_\theta \\ I_z \end{bmatrix} = -\frac{1}{2} \operatorname{Re}\left\{ \begin{bmatrix} \sigma_r & \tau_{r\theta} & \tau_{rz} \\ \tau_{\theta r} & \sigma_\theta & \tau_{\theta\tau} \\ \tau_{zr} & \tau_{z\theta} & \sigma_z \end{bmatrix} \begin{bmatrix} \dot{u}^* \\ \dot{v}^* \\ \dot{w}^* \end{bmatrix} \right\}, \tag{28}$$

where $\sigma_r, \ldots, \tau_{z\theta}$ are the stress components in the structure and superscript * denotes complex conjugate. For the case of pure moment excitation, the radial and axial displacement components are equal to zero ($u = w = 0$) [3].

$$\tau_{r\theta} = G\left(\frac{\partial v}{\partial r} - \frac{v}{r}\right), \qquad \sigma_\theta = 0, \qquad \tau_{z\theta} = G\frac{\partial v}{\partial z}. \tag{29}$$

Combining equations (28) and (29) gives

$$I_r = -\tfrac{1}{2} \operatorname{Re}\{\tau_{r\theta}\dot{v}^*\}, \qquad I_\theta = 0, \qquad I_z = -\tfrac{1}{2} \operatorname{Re}\{\tau_{z\theta}\dot{v}\} \tag{30}$$

The shear stresses in segments 1 and 2 of the stepped shaft can be calculated using equations (16), (17) and (29):

$$\tau_{r\theta}^{(1)}(r, z, t) = \sum_{n=1}^{\infty} \frac{\beta_n^{(1)} J_2(\beta_n^{(1)} r)}{k_n^{(1)} \sin(k_n^{(1)} L_1)} [c_n^{(1)} \cos(k_n^{(1)} z) + c_n^{(0)} \cos(k_n^{(1)}(z - L_1))] \, e^{j\omega t}; \tag{31}$$

$$\tau_{r\theta}^{(2)}(r, z, t) = \sum_{n=1}^{\infty} \frac{\beta_n^{(2)} J_2(\beta_n^{(2)} r)\, c_n^{(2)} \cos(k_n^{(2)}(z - L))}{k_n^{(2)} \sin(k_n^{(2)} L_2)} e^{j\omega t} \tag{32}$$

$$\tau_{r\theta}^{(1)}(r, z, t) = \left\{ \begin{array}{l} \dfrac{r}{\sin(k_0^{(1)} L_1)} [c_0^{(1)} \sin(k_0^{(1)} z) + c_0^{(0)} \sin(k_0^{(1)}(z - L_1))] \\ + \displaystyle\sum_{n=1}^{\infty} \frac{J_1(\beta_n^{(1)} r)}{\sin(k_n^{(1)} L_1)} [c_n^{(1)} \sin(k_n^{(1)} z) + c_n^{(0)} \sin(k_n^{(1)}(z - L_1))] \end{array} \right\} e^{j\omega t}, \tag{33}$$

$$\tau_{r\theta}^{(2)}(r, z, t) = \left\{ \frac{r c_0^{(2)} \sin(k_0^{(2)}(z - L))}{\sin(k_0^{(2)} L_2)} + \sum_{n=1}^{\infty} \frac{J_1(\beta_n^{(2)} r)\, c_2^{(2)} \sin(k_n^{(2)}\ (z - L))}{\sin(k_n^{(2)} L_2)} \right\} e^{j\omega t}. \tag{34}$$

Substituting equations (16), (17) and (31)–(34) into equation (30) gives the structural intensities in segments 1 and 2 of the stepped shaft.

4. NUMERICAL RESULTS AND DISCUSSIONS

A numerical example is presented in this section to assess the feasibility of the method described and also to illustrate the characteristics of dynamical response, shear stress and structural intensity fields of torsional vibration in a stepped shaft. The stepped shaft is assumed to be made of mild steel and has free–free end conditions. $R_1 = 0{\cdot}5$ m, $R_2 = 0{\cdot}25$ m, $L_1 = 1{\cdot}0$ m, $L_2 = 0{\cdot}5$ m. The dissipation loss factors of both segments are assumed to be the same of 0·001. The left end of the stepped shaft ($z = 0$) is excited by an external torque of unit magnitude ($M_0 = 1$ Nm) which resulted from a distributive surface

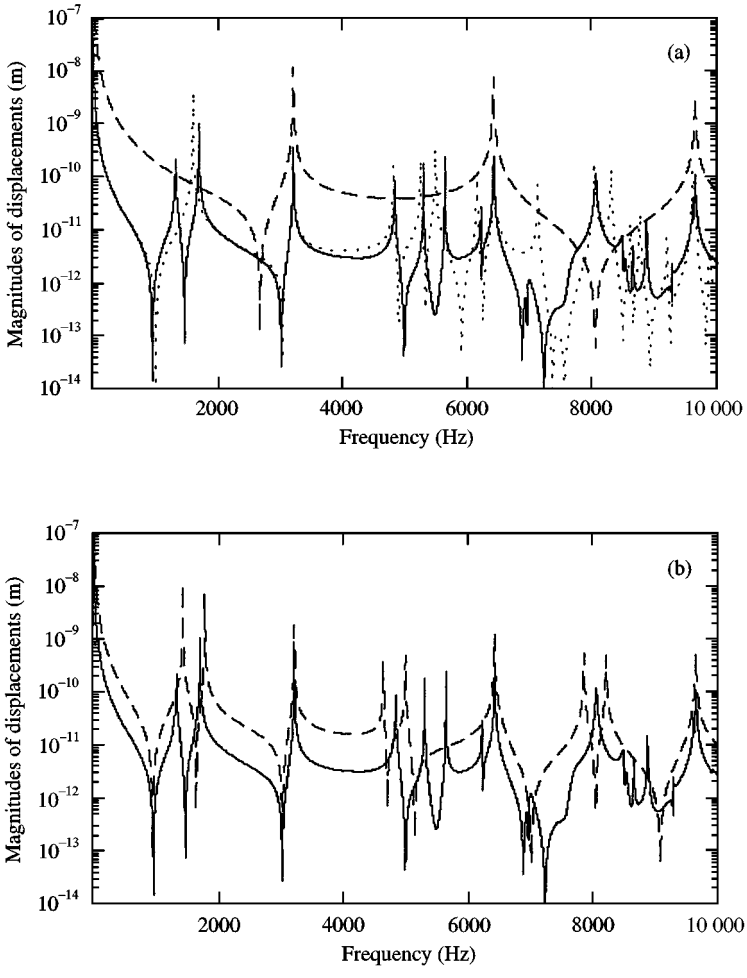

Figure 2. Magnitudes of the tangential displacements calculated at position of $(r, z) = (0{\cdot}2\text{ m}, 0{\cdot}2\text{ m})$: (a) using three-dimensional torsional vibration theory for the stepped shaft (———) and for uniform shafts (- - - - -: $(L, R) = (1{\cdot}0\text{ m}, 0{\cdot}5\text{ m})$; – – –: $(L, R) = (0{\cdot}5\text{ m}, 0{\cdot}25\text{ m})$); (b) using three-dimensional torsional vibration theory (———) and one-dimensional torsional vibration theory (– – –) respectively in the stepped shaft.

force. Numerical results showed that in a stepped shaft both the shear stresses and velocity fields are independent of the external excitation force function (that is, the expression of $\Theta_0(r)$ which may be proportional to r or $r^n (n > 1)$). This is different from the case of uniform shafts [3]. The reason is that the internal forces at the stepped joint are always non-uniform regardless of the type of external excitation force. In our calculations, a cubically distributed external surface force ($\Theta_0(r) = 3r^3/\pi R_1^6$) was assumed.

Figure 2 shows the magnitudes of tangential displacements v_1 at position of $(r, z) = (0{\cdot}2\text{ m}, 0{\cdot}2\text{m})$ in the stepped shaft and uniform shafts $(L, R) = (1{\cdot}0\text{ m}, 0{\cdot}5\text{ m})$ and $(0{\cdot}5\text{ m}, 0{\cdot}25\text{ m})$ respectively. Figure 2(a) is used to illustrate the relationship between the coupled system (stepped shaft) and the uncoupled systems (the segments) in terms of their resonance frequencies. It was found that when the resonance frequencies of the axial modes of the two-segments coincide, the stepped shaft finds its resonance. If the resonance e frequencies of the two segments do not coincide, the resonance frequency of the stepped shaft shifts

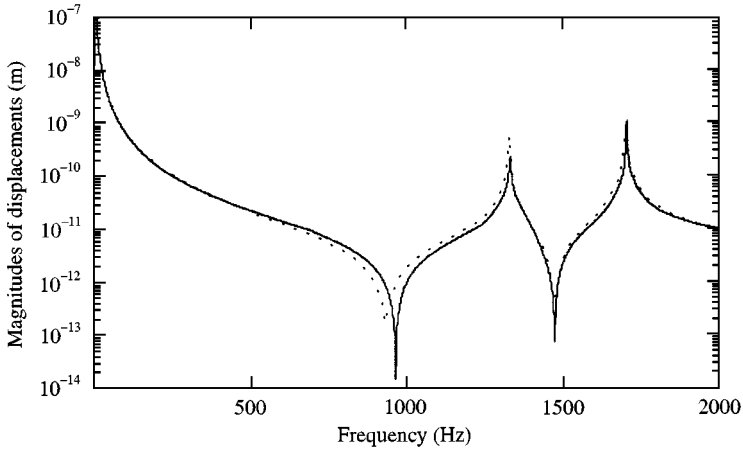

Figure 3. Magnitudes of the tangential displacement at position of $(r, z) = (0{\cdot}2 \text{ m}, 0{\cdot}2 \text{ m})$ in the stepped shaft calculated using the three-dimensional torsional vibration theory (———) and using the finite element methods (- - - - - - -).

away from that of the uncoupled segments. Figure 2(b) shows that the one-dimensional torsional vibration theory not only misses out the resonance frequencies of radial modes, but also results in a large error for the prediction of resonance frequencies of axial modes in a stepped shaft when the resonance frequencies of the two segments (in free–free end conditions) do not coincide. This is different from the case of uniform shafts where the prediction error for using one-dimensional torsional vibration theory is negligible [2].

To assess the accuracy of the present method, the finite element method (FEM) (MSC/Nastran 7·07) was used to calculate the displacement response of the stepped shaft in the low-frequency range (the high-frequency calculation has been prevented by the required mesh size and number of elements). The results from FEM and the present method are compared in Figure 3. The comparison shows a reasonable accuracy of the present method.

It is shown in equations (16), (17) and (31)–(34) that both shear stresses and tangential displacement are the sum of infinite terms. The numerical calculation, however, can only include a finite number of terms. Also the use of the method of least squares can only make the boundary conditions be exactly satisfied at a finite number of locations. Therefore, this proposed method is theoretically an approximate numerical method. The approximate error is a function of the base function and fitting location numbers. Figures 4 and 5 show the magnitude values of tangential displacements and shear stresses $\tau_{z\theta}$ at different resonance frequencies for different base function and fitting location numbers (S and M) respectively. During the calculations, $P = Q = S$ and $M = N$ (because $R_1 = 2R_2$) were used. The frequency of $f = 3218$ Hz is the third resonance frequency of the stepped shaft and it coincides with the second symmetric axial modal frequency of segment 1 and the first antisymmetric axial modal frequency of segment 2. The frequency of $f = 5310$ and 5652 Hz are the fifth and sixth resonance frequencies of the stepped shaft and at which the symmetric and antisymmetric radial modes are respectively present in segment 1. It can be seen that the approximation error depends on frequency. If the resonance frequency of stepped shaft coincides with the resonance frequencies of both segments, an accurate calculation can be made by using small numbers of base functions and fitting locations (both S and M are small). Otherwise (even for axial modes), more base functions and fitting locations are required. The required numbers of base functions and fitting location are different at different resonance frequencies. The numerical results also showed that at non-resonance

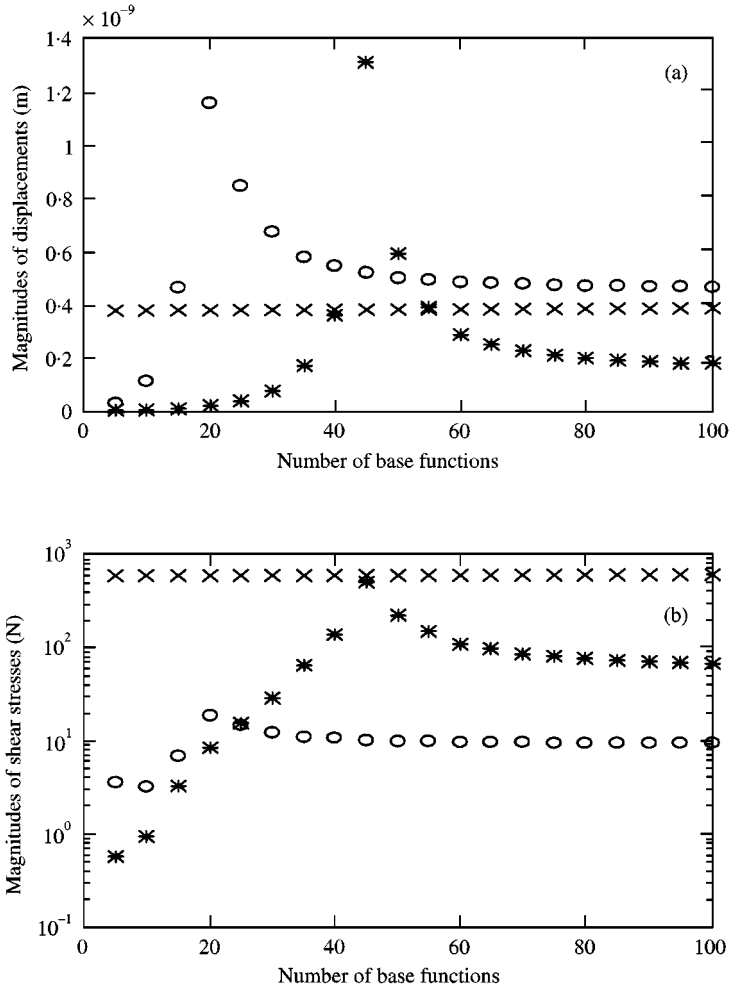

Figure 4. Magnitudes of tangential displacements (a) and shear stresses $\tau_{z\theta}$ (b) at the resonance frequencies of $f = 3218$ Hz ($\times$), 5310 Hz (O), 5652 Hz (*) on the position of $(r, z) = (0{\cdot}2\,\text{m}, 0{\cdot}2\,\text{m})$ in the stepped shaft.

frequencies accurate results can be obtained by using small numbers of base functions and fitting locations.

Figures 6 and 7 shows the contour plots of two-dimensional displacements and shear stresses $\tau_{z\theta}$ at the resonance frequencies of $f = 3218$ and 8876 Hz respectively. Since the displacement and shear stress distribution are independent of θ, these contour plots give the vibration patterns for any lateral cross-section of the stepped shaft. At $f = 3218$ Hz, the stepped shaft vibrates in an axial mode and the vibration pattern can be predicted with a negligible error using one-dimensional torsional vibration theory. At $f = 8876$ Hzz, the vibration pattern is complicated and its analyses must be made using three-dimensional torsional vibration theory.

Figures 8 and 9 show the structure intensity vector fields at resonance frequencies of $f = 3218$ and 8876 Hz. It can be seen that the structural intensity is not uniformly distributed in the radial direction. Most input power is dissipated in segment 1. This is because the stepped shaft is in free–free end conditions and the two segments have the same

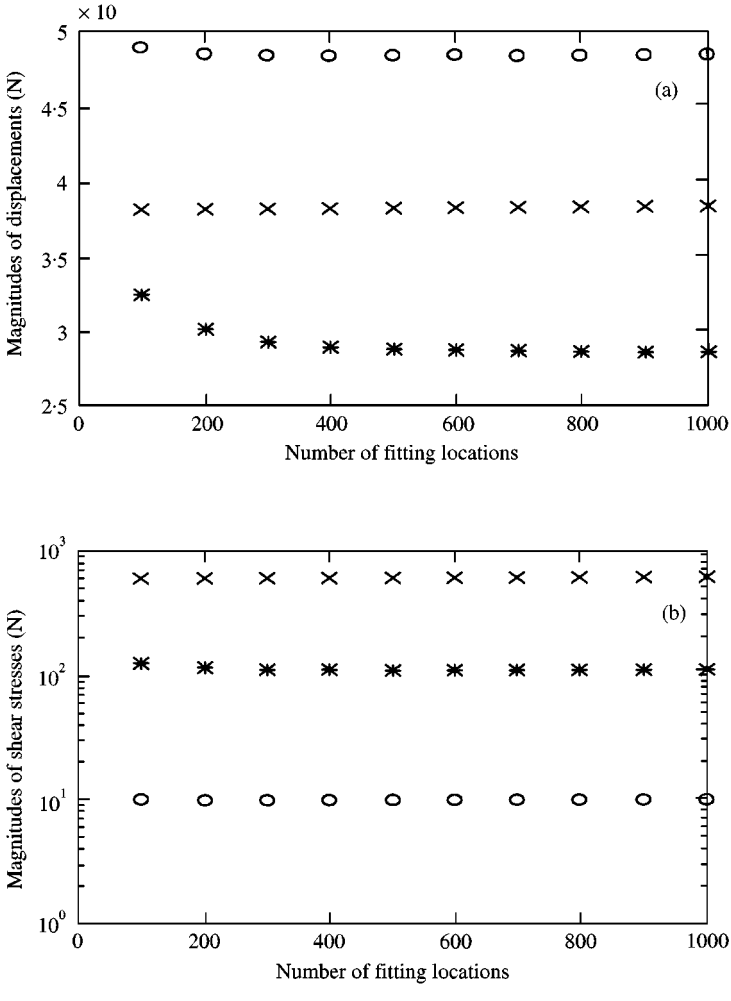

Figure 5. Magnitudes of tangential displacements (a) and shear stresses $\tau_{z\theta}$ (b) at the resonance frequencies of $f = 3218$ Hz ($\times$), 5310 Hz (O), 5652 Hz (*) on the position of $(r, z) = (0{\cdot}2\,\text{m}, 0{\cdot}2\,\text{m})$ in the stepped shaft.

dissipation loss factors. For an axial vibration mode ($f = 3218$ Hz), the radial intensity component is very smaller than the axial one at the all the locations and the structural intensity vector is in a simple distribute pattern. For a radial vibration mode ($f = 8876$ Hz), intensity vortices are present in the intensity vector field. These two figures indicate that the prediction of structural intensity distribution at any frequency in a stepped shaft must be made based on a three-dimensional mathematical model.

5. CONCLUSIONS

In this paper, a method is outlined for calculating the dynamic response and shear stresses of torsional vibration in three-dimensional stepped shafts. By using the eigenfunctions of torsional vibration in uniform cylindrical rods as the base functions and applying the method of least squares to the boundary conditions, this method is able to

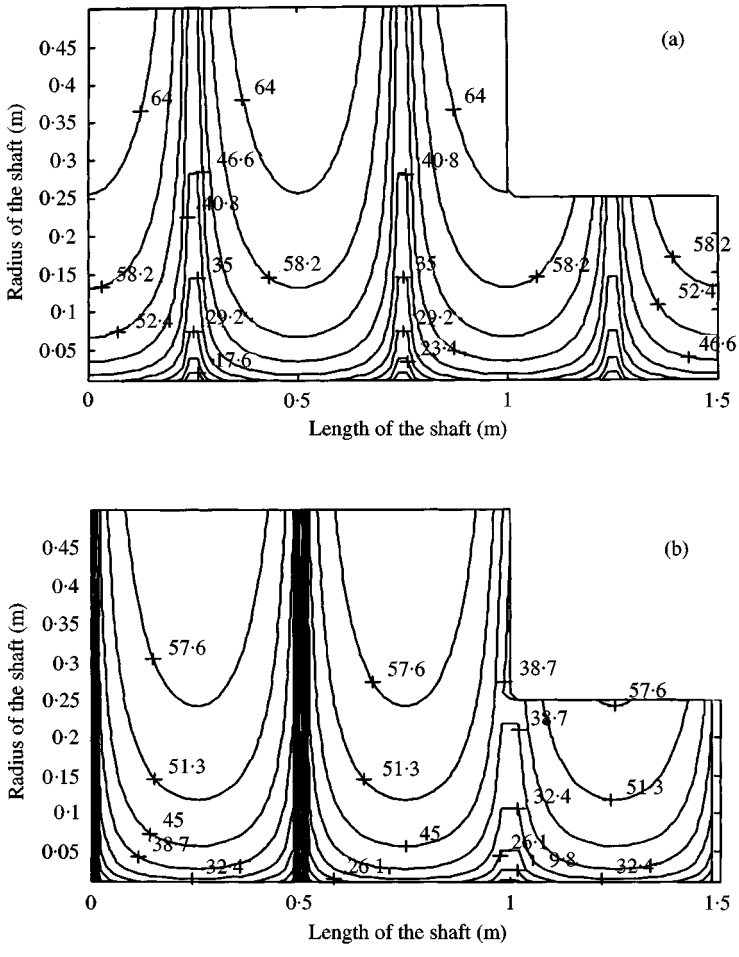

Figure 6. Magnitude contours of the displacements (a, dB re 1×10^{-12} m) and shear stresses $\tau_{z\theta}$ (b, dB re 1 N) in the stepped shaft at the resonance frequency of $f = 3218$ Hz.

provide detail and accurate information of the dynamic response, shear stresses and structural intensity in three-dimensional finite stepped shafts. Although in this paper only a stepped shaft of two finite cylindrical rods with free–free end conditions is taken as an example, this proposed method can be easily applied to the stepped shafts consisting of many finite cylindrical rods or having other boundary conditions.

Work in progress includes the study of stress concentration near the stepped joint [13] and experimental verification.

ACKNOWLEDGMENT

Financial support for this work from the Australian Research Council is gratefully acknowledged.

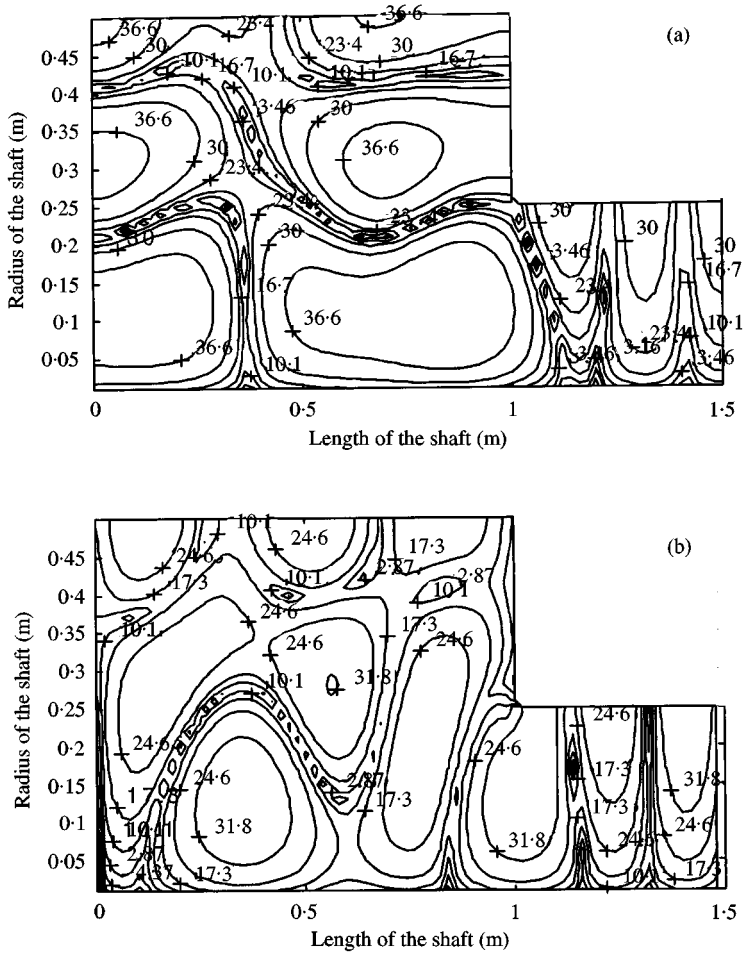

Figure 7. Magnitude contours of the displacement (a, dB re 1×10^{-12} m) and shear stress $\tau_{z\theta}$ (b, dB re 1 N) in the stepped shaft at the resonance frequency of $f = 8876$ Hz.

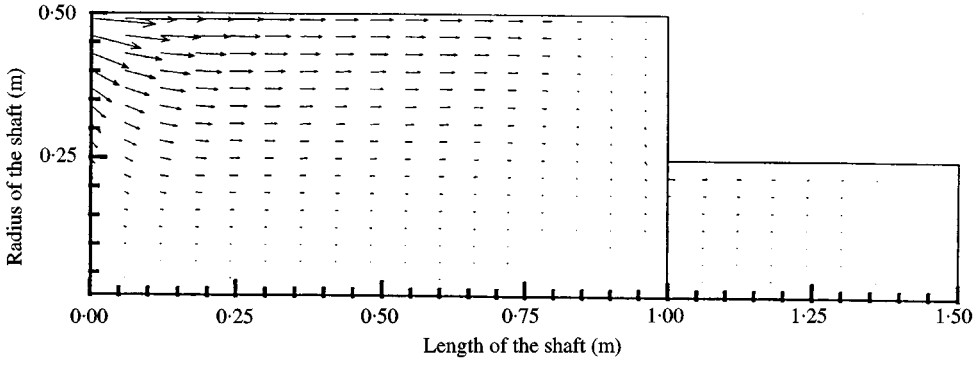

Figure 8. Structural intensity vector field at the resonance frequency of $f = 3218$ Hz.

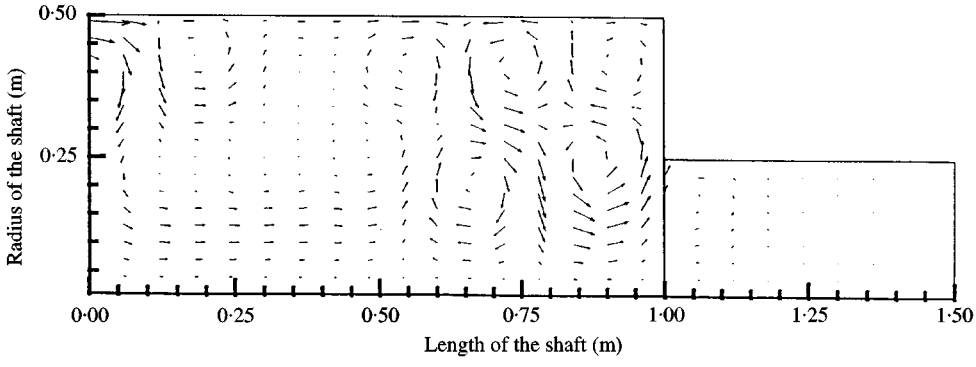

Figure 9. Structural intensity vector field at the resonance frequency of $f = 8876$ Hz.

REFERENCES

1. D. J. GORMAN 1975 *Free Vibration Analysis of Beams and Shafts*. New York: John Wiley & Sons.
2. A. W. LEISSA and J. SO 1995 *Journal of the Acoustical Society of America* **98**, 2122–2135. Comparisons of vibration frequencies for rods and beams from one-dimensional and three-dimensional analysis.
3. J. Q. PAN and J. PAN 1998 *Journal of the Acoustical Society of America* **103**, 1475–1482. Structural intensity of torsional vibration in solid and hollow cylindrical bars.
4. W. JOHNSON, B. A. AULD and E. SEGAL 1996 *Journal of the Acoustical Society of America* **100**, 285–293. Trapped torsional modes in solid cylinders.
5. T. TSUJI, T. SHIBUYA, T. KOIZUMI and K. TAKAKUDA 1985 *Bulletin of the JSME* **28**, 2547–2552. Torsional problem for bonded rods.
6. T. TSUJI, N. NODA, T. SHIBUYA and T. KOIZUMI 1991 *Bulletin of the JSME* **33**, 474–479. Stress singulrity in a step bar under impact torsion.
7. T. TSUJI, N. NODA, T. SHIBUYA and T. KOIZUMI 1991 *International Journal of Solids and Structures* **27**, 1059–1071. Stress singularity in torsion problem for bonded bars.
8. Y. Y. KIM and J. H. KIM 1995 *Quarterly Journal of Mechanics and Applied Mathematics* **48**, 517–530. Stress analysis of a stepped shaft under remote torsion.
9. G. N. WATSON 1962 *A Treatise on the Theory of Bessel Functions*, Cambridge: Cambridge University Press, second edition.
10. D. G. REES 1987 *Foundations of Statistics*. London: Chapman & Hall.
11. G. PAVIC 1987 *Journal of Sound and Vibration* **115**, 405–422. Structural surface intensity: an alternative approach in vibration analysis and diagnosis.
12. W. MAYSENHOLDER 1990 *Acoustica* **72**, 166–179. Rigorous computation of platewave intensity.
13. J. PAN, J. Q. PAN and R. S. MING 1999 *Proceedings of the 6th International Congress on Sound and Vibration, Technical University of Denmark, Lyngby 5–8 July*, 1999, 2075–2081. Vibration in a three-dimensional step shaft.